PCCP

Accepted Manuscript

ROYAL SOCIETY OF CHEMISTRY

www.rsc.org/pccp

Cite this: DOI: 10.1039/c0xx00000x

www.rsc.org/xxxxxx

ARTICLE TYPE

Gold nanoparticles interactions mediated by captopril and S-nitrosocaptopril. Effect of manganese ions in mild acid medium

Emilia Iglesias*[a] and Rafael Prado-Gotor[b]

Received (in XXX, XXX) Xth XXXXXXXXX 20XX, Accepted Xth XXXXXXXXX 20XX

DOI: 10.1039/b000000x

We report herein results on reactivity and assembly of citrate-capped gold nanoparticles (AuNPs) mediated by captopril (cap) and S-nitrosocaptopril (NOcap), two angiotensin converting enzyme inhibitors and antihypertensive agents. The results were compared with that of cysteine (Cys), a thiol-containing amino acid found in plasma. The interparticle interactions were characterized by monitoring the evolution of the surface plasmon resonance band using the spectrophotometric method. The original gold nanoparticles were efficiently modified by small amounts of Mn^{+2} ions, which are adsorbed to the surface of 15.4 nm citrate-capped gold nanoparticles, giving rise to manganese-gold nanoparticles (Mn-AuNPs) that, in mild acid medium, have proved to be highly sensitive and rapid colorimetric detection method for thiols. Depending on the concentration the Mn^{+2} ions the aggregation of AuNPs can be rapidly induced. The kinetics of assembly process has been studied. Good first-order kinetics has been observed, with the exception of captopril-mediated nanoparticles aggregation at low concentration of either cap or acid. In aqueous 10 mM acetic acid of colloidal gold nanoparticles the rate of Cys-mediated assembly results more than 20-fold faster than pure AuNPs and concentrations of Cys as low as 34 nM can be detected in less than 40 min under conditions of stable Mn-AuNPs. Similar effects were observed with cap or NOcap. The assembly-disassembly reversibility is shown with cap and NOcap and depends highly on pH.

Introduction

Noble metallic nanoparticles, especially gold nanoparticles, have unique properties of enormous interest for biological and chemical sensing applications.[1-5] The fact that, AuNPs absorb and scatter light at their surface plasmon resonance (SPR) band, makes nanometric gold as a valuable optical probe for detection methods. The optical properties of AuNPs depend strongly on the surface chemistry and on the interparticle interactions.[6] Gold nanoparticles form stable chemical bonds with S- and N-containing groups. Consequently, small organic ligands may be conveniently attached to the surface of AuNPs through their thiol or amine functionalities.

Localized surface plasmon resonance peaks of gold nanoparticles are strongly governed by their size, shape and the dielectric constant of the surrounding medium.[3] The preparation of colloidal spherical AuNPs with diameters of 5-50 nm can be done from the reduction of $HAuCl_4$ with sodium citrate in boiling water, according to the well-known Turkevich method.[7, 8] The procedure affords well-dispersed colloidal gold aqueous solutions of red colour, whereas surface plasmon coupling results in a colour change from red to blue at nanomolar concentration.[3,9,10] Encapsulation of AuNPs by adsorption or binding organic molecules, such as thiols, on the particle surface and subsequent cross-linking at binding sites of the encapsulating shells are of crucial importance in determining the colour change, which is the basis of colorimetric methods that use SPR sensors.

Thiols are among the organic molecules most studied in this sense. Homocysteine (Hcys) rapidly adsorbs to AuNP surface *via* –S-Au bond formation by displacing the original citrate molecules that capped gold surface; the process is followed by NPs assembly and the interparticles reactivity is accelerate by the addition of electrolytes, as well as, by lowering the pH.[11] Cysteine (Cys) interacts also with gold nanoparticles, but the SPR band evolution shows a much slower reaction rate than Hcys, being necessary ~10 h to see the maximum change.[12] The presence of 1 mM Cu^{+2} drastically enhances the rate of gold nanoparticles aggregation.[13] Glutathione (GSH) is even less reactive than Hcys or Cys. The simultaneous presence of GSH and 40 mM of sodium nitrate yields a quasi-stable state of AuNPs whose solution remains of red-colour, contrarily to that observed with other thiols, a fact that serves as a colorimetric method for GSH analysis with very low detection limit of 0.5 μM.[14] Nevertheless, in organic solvents such as THF, the aggregation of gold organosols can be controlled using GSH, a pH sensitive biomolecule, as a molecular linker of the 'parent' gold nanoparticles.[15] Penicillamine (PEN) and N-acetylpenicillamine (NAP) modify gold nanoparticles in a few seconds at very low pH (1.9 and 1.7, respectively). From isothermal titration calorimetry measurements the equilibrium constants for the thiol binding to gold surface have been determined of the order 10^7 M^{-1}

and near 40 or 60% of gold surface coverage by PEN or NAP, respectively, was estimated.[16]

Reeves *et al*.[17] carried out a systematic and detailed study on the ability of small molecules that include thiol-, amine-, or carboxyl-functionalities, or their combinations, to bind and aggregate gold nanoparticles at variable pH. The main goal of this study is to present models for mechanisms of aggregation of colloidal gold solutions, including the possible reduction in zeta potential that leads to nanoparticles instability and bridging linkers from one nanoparticle to another, or even by forming the so-called surface micelles.[18] The interesting study of Reeves shows that the as-synthesized colloidal gold solutions have minimal absorption in the red spectral region despite considerable variation in the pH of the solution ranging from pH 3.1 to 11.2, and after as long as 24 h incubation, which evidences the unaggregated nanoparticles solution. The study also verifies that the protonation state of the carboxylic groups in general and citrates in particular plays a crucial role in driving the aggregation kinetics. Consequently, low (acidic) pH values accelerates the aggregation rate and, on the other hand, the replacement of adsorbed anionic citrates with molecules not containing carboxylate groups or bearing positively charged groups, such as amino acids, favours nanoparticle aggregation.

Our aim in this research work was to find suitable conditions of AuNPs aggregation mediated by captopril (cap) and S-nitrosocaptopril (NOcap). Therefore, we carried out a systematic study of the interaction of cap and NOcap with citrate stabilized gold nanoparticles, and the results were compared with the well-studied Cys. Scheme 1 shows the corresponding molecular structures along with that of other thiols already studied and their pK_a values.[19-21] NOcap is a nitric oxide donor and NO is a biological transmitter that mediates in vasodilation and in angiogenesis.[21,22] By coupling the exciting properties of AuNPs with paramagnetic properties of Mn^{+2} ions we present new sensors of improved response time in aqueous acetic acid medium. Consequently, the interactions of AuNPs with both acetic acid (AcH) and Mn^{+2} ions have been analysed. The experimental data verify the models of gold nanoparticles assembly proposed by Reeves. In this sense, the high efficiency of Mn^{+2} ions in reducing zeta potential of citrate-capped gold nanoparticles strongly affects their stability even at neutral pH. In the same line, the tuned protonation of carboxyl citrate by the presence of small amounts of AcH accelerates the rate of nanoparticles assembly promoted by bridging linkers, such as Cys, cap or NOcap, from one nanoparticle to another.

Experimental

Materials. Captopril, cysteine and other chemicals, such as hydrogen tetrachloroaurate trihydrate ($HAuCl_4.3H_2O$), sodium citrate, manganese(II) chloride, acetic acid, sodium nitrite were used as received from Sigma-Aldrich Chemicals.

S-Nitrosocaptopril was synthesized by mixing 300 µL of $NaNO_2$ 20 mM with 800 µL of cap 7.5 mM into 1.9 mL of acetic acid 6.7 mM. The rapid NOcap formation is observed by the evolution of the absorption band at 332 nm.[21] Solutions of NOcap were used within the next 4 or 5 hours; nevertheless, at low temperature it is stable during several days.

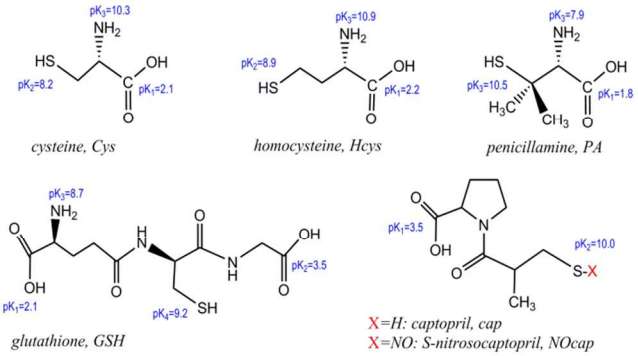

Scheme 1. Molecular structure of model organothiols and the pK_a values of the ionisable carboxyl-, thiol-, and amino-groups (notice that the ionisable amine group must be $–NH_3^+$)

Gold nanoparticles were prepared following standard procedures.[7,8] Briefly, aqueous $HAuCl_4$ was first heated to boiling and followed by a rapid addition of an excess of aqueous sodium citrate. The characterization of gold nanoparticles capped by citrate shells resulted in [AuNPs]=2.82 nM of diameter 15.4 nm that show the maximum wavelength absorption at 520 nm. The Mn-AuNPs were prepared by diluting aliquots (30 - 200 µL) of 4.0 mM Mn^{+2} ($MnCl_2$) into 1 mL final volume of citrate capped AuNPs 0.85 nM, resulting in final concentrations of Mn^{+2} varying between 0.12 to 0.8 mM.

Water was firstly deionised and subsequently twice distilled (the first distillation over potassium permanganate).

Methods. The UV-Visible (UV-vis) spectra and kinetics were recorded with a Kontron-Uvikon double beam spectrophotometer fitted with thermostated multicell holders. Spectra were collected over the range 200-800 nm. In a typical experiment, the stock solution of nanoparticles was diluted with distilled water to reach a final colloidal gold concentration of 0.85 nM. Quartz cuvettes of 1 cm path-length and 1.4 mL capacity were used. In studying the kinetics of the evolution of the surface plasmon resonance band of AuNPs, measurements of absorbance (A) *versus* time (t) were recorded and fit to the first-order integrated rate equation, $A=A_\infty-(A_o-A_\infty)\cdot exp(-k_o t)$, unless otherwise indicated. The non-linear regression analysis of A-t data gives k_o, A_o, and A_∞ as optimizable parameters, with k_o being the pseudo-first order rate constant and A, A_o, and A_∞ being the absorbance values at times t, zero, and at the end of the reaction. All experiments were conducted at 25 ºC

The pH was measured with a Crison 2001 pH-meter equipped with a GK2401B combined glass electrode and calibrated using commercial buffers of pH 4.01, 7.02, and 9.26 (Crison).

Transmission electron microscopy (TEM) was carried out using a JEOL JEM 1010 electron microscope operating at an acceleration voltage of 100 kV and equipped with a Mega View III camera controlled with Analysis software. Samples of TEM analysis were prepared by placing drops of gold colloidal solutions onto a carbon-coated copper grid sample holder followed by evaporation in air at room temperature. The reported TEM images are representative on the entire grid sample.

The ζ-potential was determined with a Malver Zetasizer Nano-ZS90. Measurements were recorded at 25 ºC as a function of Mn^{+2} ions concentration. Values of ζ-potential were automatically calculated from electrophoretic mobility based on

Smoluchowski equation.

Results and Discussion

1. Manganese-gold nanoparticles, Mn-AuNPs. Figure 1 (a and b) shows the UV-vis spectra comparing the SPR band evolution for the as-synthesized solutions of gold nanoparticles in 10 mM AcH upon the addition of 0.20 mM of Mn^{+2} ions. Aqueous solution of AuNPs exhibits a characteristic absorption band at 520 nm that corresponds to the plasmon resonance band for well-dispersed spherical AuNPs. In 10 mM acetic acid the spectra remains practically unchanged (spectra recorded during 2 h, Fig 1(a)) and the corresponding TEM image, shown in Figure 1(c), does not indicate any aggregation effects.[23] After addition of Mn^{+2} the intensity of SPR band goes down bit while a new plasmon band (600-800 nm) appears, Fig 1(b).

In the absence of acetic acid, the spectrum of aqueous AuNPs recorded at 0.20 mM of Mn^{+2} remains unchanged during at least 30 min; by doubling the Mn^{+2} concentration, a very slow increase of the absorbance in the range 600-800 nm is clearly observed, whereas at $[Mn^{+2}]$=0.80 mM the new plasmon band centered at ~672 nm develops is less than 5 min, see Figure 2.

Figure 3(a) shows comparative absorbance-time data of SPR band time evolution of AuNPs under three experimental conditions of (i)10 mM AcH, in where no appreciable absorbance increase has been observed during 80 min; (ii)10 mM AcH and 0.12 mM Mn^{+2}, in which medium the nanoparticles seems to be also stable in, at least, 100 min, and (iii)10 mM AcH containing 0.20 mM Mn^{+2}, in which medium noticeable changes can be clearly observed. Figure 3(b) shows the absorbance increase at 672 nm as a function of time for $[Mn^{+2}]$ equal to 0.81; 0.61, and 0.40 mM. At 0.81 mM, the blue colour of gold colloidal solutions develops in less than 5 min, whereas at half this concentration, the colour change is much slower, being unappreciable even in 1 h, but the addition of 10 mM acetic acid accelerates strongly the process as it is shown in Figure 3(c) by the corresponding TEM image that indicates complete aggregation in less than 40 min.

Data of absorbance (A) versus time (t) fit perfectly the first-order integrated rate equation, and the observed rate constant, k_o, of the self-assembly process were determined as a function of Mn^{+2} ions concentration. The results are listed in Table 1 and solid lines in Figure 3 (a and b) show the fit of the model to the experimental data.

The analysis of these results indicates negligible aggregation of gold nanoparticles in 10 mM AcH aqueous solutions in the absence or in the presence of 0.12 mM of Mn^{+2} and in the timeframe of the observation. By contrast, working with double the $[Mn^{+2}]$, a new absorption band at longer wavelengths evolves with time due to nanoparticles assembly. The extension of aggregation increases with $[Mn^{+2}]$; a fact which is further corroborated by the effect of $[Mn^{+2}]$ on the absorbance readings at 672 nm at infinite time, see the last column in Table 1.

An estimation of the variation of k_o with $[Mn^{+2}]$ leads to an exponential increase of the rate of the gold nanoparticles assembling process according to equation (1), i.e. proportional to four-degree of $[Mn^{+2}]$.

$$k_o = k\,[Mn^{+2}]^4 \qquad (1)$$

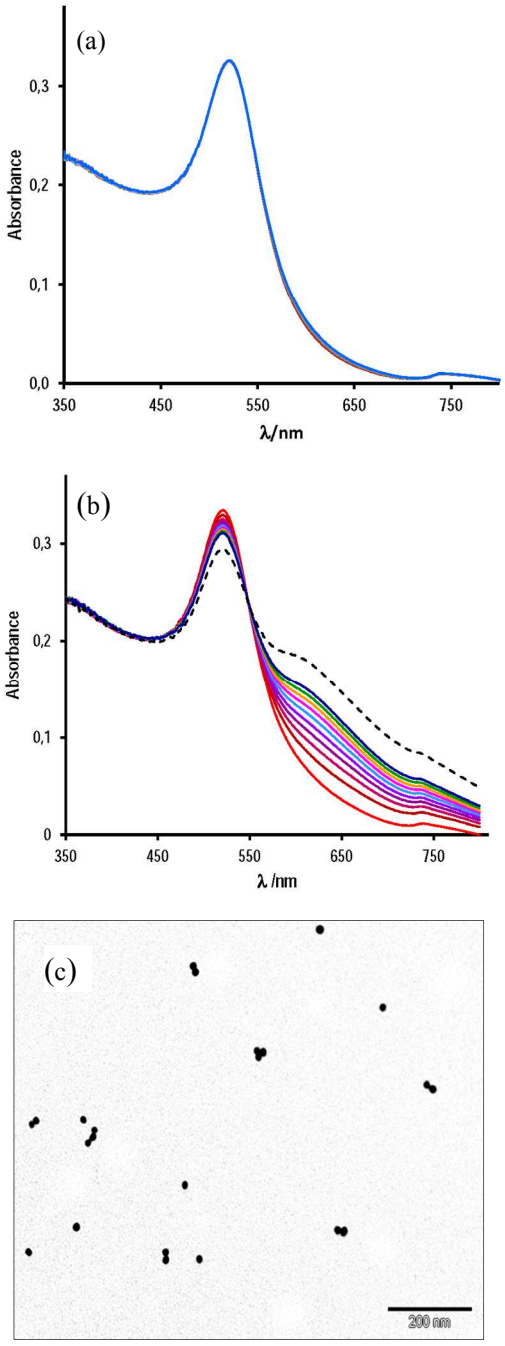

Figure 1. UV-vis spectra of AuNPs (0.85 nM) in the presence of 10 mM AcH at (a)$[Mn^{+2}]$=0, and (b)$[Mn^{+2}]$=0.20 mM; scans at 6 min interval during 120 min; scan (---)at 120 min; (c)TEM image of AuNPs under conditions of (a) after 90 min of mixing the reactants.

This fact suggests a large efficiency of Mn^{+2} ions in the interaction with AuNPs to promote self-assembly. The rate constant of the assembly process was determined as $k=(1.31\pm0.01)\times10^{11}$ $M^{-4}s^{-1}$ in the presence of 10 mM acetic acid and of $k=(1.34\pm0.04)\times10^{10}$ $M^{-4}s^{-1}$ in the absence of acetic acid. The effect of acetic acid, in the sense of modulating the protonation of citrate, explains these results because, lowering the net negative charge of NPs leads to a compression of the electrical double layer that surrounds AuNPs, which increases the self-assembly rate.

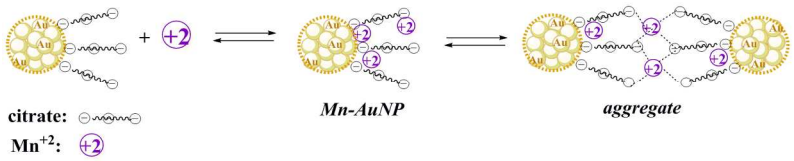

Scheme 2. Schematic representation of interfacial interactions for Mn^{+2} -mediated assembly of citrate-capped gold nanoparticles.

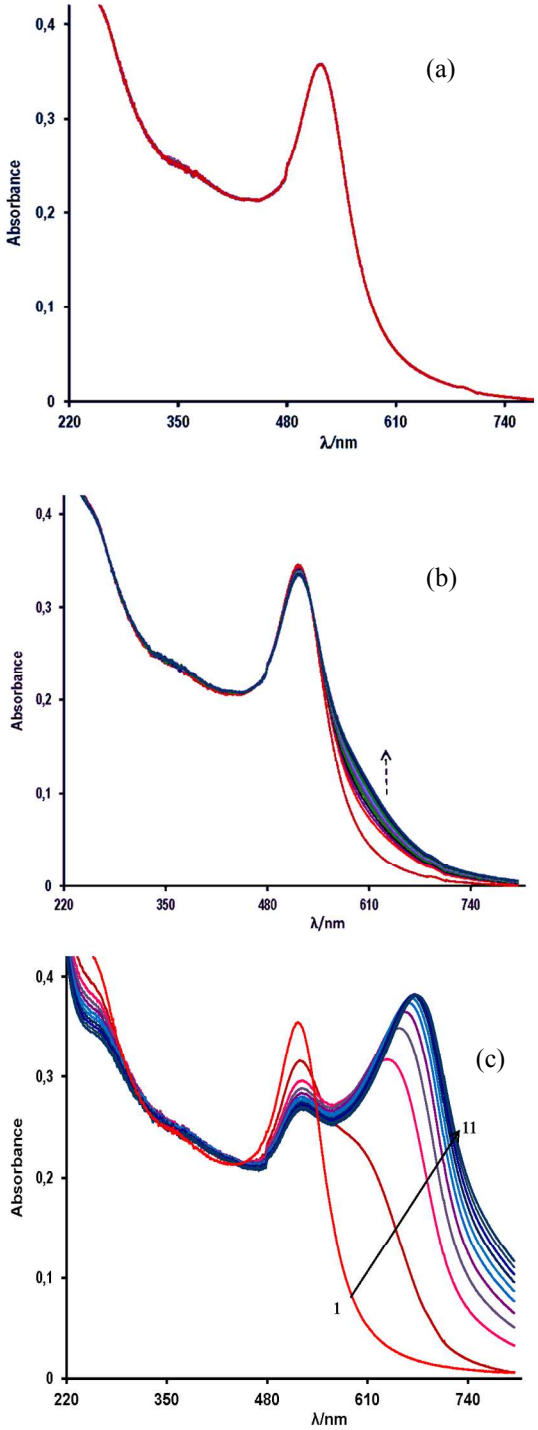

Figure 2. UV-vis spectra of aqueous solutions of AuNPs at (a)[Mn^{+2}]=0.20 mM, scans each 2 min during 20 min; (b)[Mn^{+2}]=0.40 mM, scans at 3 min interval during 30 min, and (c)[Mn^{+2}]=0.81 mM, scans at 2.5 min interval during 25 min, scan 1 is due to gold nanoparticles solution in the absence of Mn^{+2} ions.

Table 1. Experimental conditions and values of k_o and of the maximum absorbance change (ΔA) of aqueous solutions of 0.85 nM gold nanoparticles observed during at least 100 min.

[AcH]/mM[(a)]	[Mn^{+2}]/mM	λ_{max}/nm	$k_o/10^{-3}$ s^{-1}	ΔA [(b)]
---	0.20	610	not measurable	~0
10	--	610	not measurable	~0
10	0.12	610	not measurable	0.025[(c)]
10	0.20	610	0.30±0.01	0.186
10	0.40	610	3.60±0.09	0.236
10	0.61	610	18.1±0.2	0.317
---	0.40	672	0.180±0.001	0.137
---	0.61	672	1.58±0.01	0.300
---	0.80	672	5.60±0.01	0.381

[(a)]Acetic acid; [(b)]ΔA (=A_∞-A_o); [(c)]in 100 min

In aqueous solution the highest value determined for the rate constant of a diffusion-controlled process, corresponds to the neutralization of H^+ and OH^-, $k_n=1.5\times10^{11}$ $M^{-1}s^{-1}$, explained by Grothus's mechanism.[24] The value estimated in this study can be understood by considering the high number of charges of approaching NPs.

The pH of 10 mM acetic acid aqueous solution has been measured as 3.30; aqueous solution of 0.85 nM AuNPs has a pH of 6.20, whereas the pH of 0.85 nM AuNPs in 10 mM acetic acid was measured as 4.40. As the pK_a of acetic acid is very close to the pK_2 and lower than the pK_3 of citric acid (pK_1=3.1, pK_2=4.8, and pK_3=6.4), the addition of acetic acid may reduce the negative charge of citrate-capped gold NPs. The appearance of red-shifted new band results from the coupling of the plasmon absorption of AuNPs assisted through self-assembly. For explaining the self-assembly process, two main factors can be considered. First, adsorption of Mn^{+2} reduces the negative charge of nanoparticles and, second, the carboxylate groups of citrate-capped neighbouring AuNPs are capable of complexation Mn^{+2} ions with the concomitant crosslinked particle networks, Scheme 2.

We measured the ζ-potential of AuNPs as a function of the concentration of Mn^{+2} ions. The results are shown in Figure 4, along with that determined by Murph *et al.*[25] for gold nanoparticles slightly higher, 20 nm. Our results indicate that in 10 mM AcH, the addition of 0.12 mM Mn^{+2} ions increases the ζ-potential from -33 mV to -29.4 mV. In spite of this small variation of the surface charge of AuNPs, the rate of self-assembly due to the presence of bridging linkers, such as Cys, cap, or NOcap, is dramatically increased as we will show in the next sections. On the other hand, and contrary to that observed by Murph *et al.*, higher concentrations of Mn^{+2} rapidly yields to unstable AuNPs: the ζ-potential at [Mn^{+2}]=0.8 mM, measured just after adding Mn^{+2}, was -20.5 mV, but increases with time (blue solution) to achieve ζ-potential values close to that accepted for neutral particles. This observation are in agreement with the

kinetic results depicted either in Figure 2(c) or 3(b) on the effect of 0.8 mM Mn^{+2}, under whose experimental conditions, the assembly of AuNPs is very significant in only 5 min.

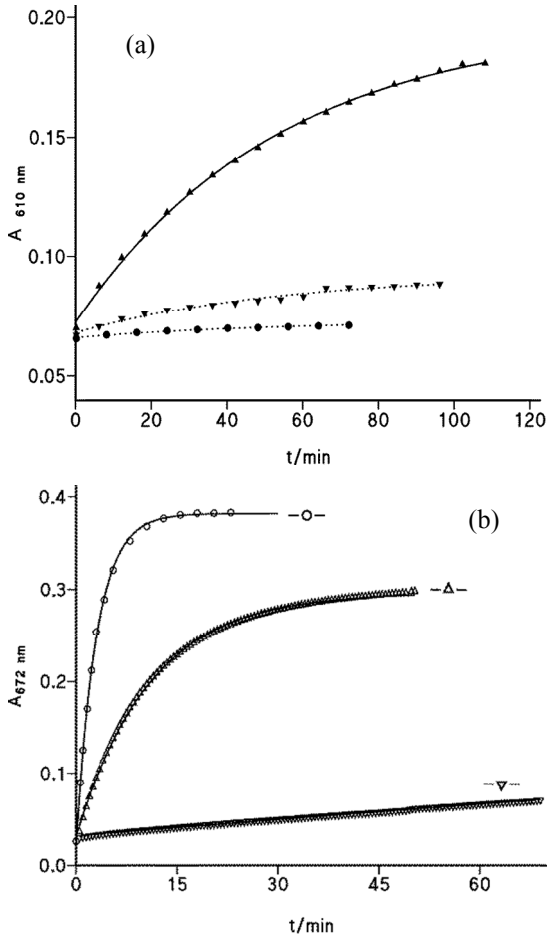

Figure 3.Absorbance versus time for aqueous AuNPs in (a)(●)10 mM AcH; (▼)10 mM AcH and $[Mn^{+2}]$=0.12 mM, and (▲)10 mM AcH and $[Mn^{+2}]$=0.20 mM; (b)(●)the uppermost curve $[Mn^{+2}]$=0.81 mM; (▲) $[Mn^{+2}]$=0.61mM, and (▼)the lowest curve $[Mn^{+2}]$=0.40mM; (c)TEM photograph of AuNPs in 10 mM acetic acid and 0.40 mM Mn^{+2} ($MnCl_2$) after 40 min incubation.

The stability of gold nanoparticles in aqueous medium depends on the protecting capped shell of citrates that surround gold-nanoparticles by an electrical double layer. This layer contains the charges on the nanocrystal surface and the counterions that serve to protect the nanoparticles from aggregation. The presence of Mn^{+2} ions reduces the net charge of citrate-capped gold nanoparticle, due to the ions complexation by the citrate-carboxylates. The effect increases with $[Mn^{+2}]$ and in the same extent the electrical double layer results compressed, which favours the interparticle interaction. As evident, when Mn^{+2} ions are added to a solution of citrate capped AuNPs, the rate of particle aggregation increases with increasing $[Mn^{+2}]$. The citrate anions have a dual role as stabilising agents for the gold core and as ligands to complex the manganese ions.

In the next sections we are going to demonstrate that stable Mn-AuNPs are improved sensors towards thiols.

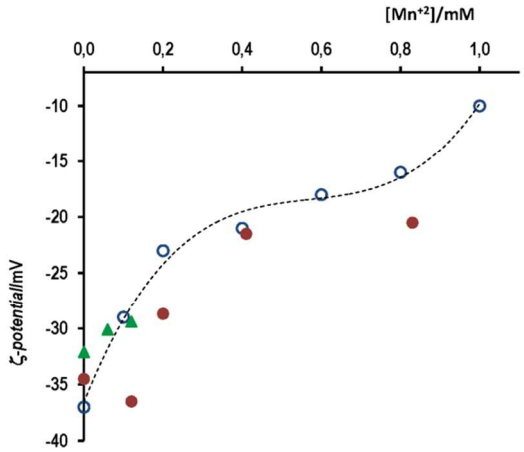

Figure 4.Variation of the ζ-potential of AuNPs as a function of $[Mn^{+2}]$, (▲)in the presence of 10 mM AcH; (●)no AcH, and (○)Murph's data for AuNPs of 20 nm size.

2. Irreversible Cys-mediated assembly of gold nanoparticles.

Thiol-containing amino acids, such as cysteine (Cys), were found to react with AuNPs through the strong covalent bonds between -SH group of Cys and gold. Therefore, AuNPs-based colorimetric detection has been used to detect Cys from the color change in the Cys-mediated assembly of AuNPs or gold nanorods.[12,13,26] The main disadvantage of these detection methods was the rather long time required in the process.

Figure 5(a) presents the time evolution of UV-vis spectra of AuNPs solutions at 10 mM acetic acid in the presence of 34 μM of Cys. The increase absorbance at long-wavelength (λ_{max}~660 nm) is completed in less than 50 min, whereas a small decrease in the short-wavelength band (~520 nm), typical of AuNPs solution (the lowest red curve), also occurs. Spectral changes are accompanied by a red-to-blue color change that can be observed with the naked eye. The reaction spectra of the same sample in the absence of AcH recorded during 1 h hardly varies; in fact, the half-live time of the process can be estimated from the work of Zhang *et al.*[12] as long as 4 h. By contrast, the Cys-mediated assembly of AuNPs is much more rapid in the presence of 0.12 mM Mn^{+2} ions, under whose conditions only 5 min is enough to clearly observe the total time evolution of the SPR band.

Figure 5(b) displays comparative data of the absorbance increase at 660 nm as a function of time for different experimental conditions. Data of A-t fit the first-order integrated rate equation and values of the observed rate constant, k_o, are listed in Table 2. As it can be seen, the rate constant of Cys-mediated AuNPs aggregation in 10 mM AcH solution is more than 20-fold faster

than that measured in aqueous solutions of AuNPs. The effect of [Cys] is small and does not show first-order dependence; notice that Cys is introduced in excess, e.g. at 17 μM there are about 20000 molecules/gold nanoparticle. Under the same experimental conditions of [Cys] and [acetic acid], the addition of 0.12 mM of Mn^{+2} ions multiplies by ~6 the rate of nanoparticles aggregation. When small amounts of AcH and Mn^{+2} ions are added to the aqueous colloidal gold solutions, concentrations of Cys as low as 34 nM can be detected and after incubation times as short as 40 min.

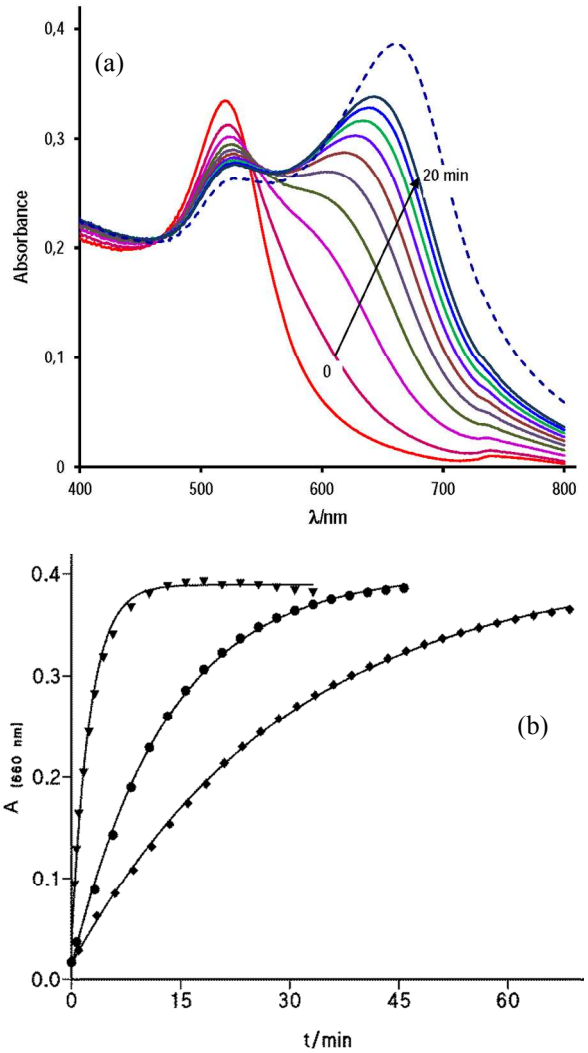

Figure 5. (a)UV-vis spectra of AuNPs at 10 mM AcH and 34 μM of cysteine recorded as a function of time; the red scan corresponds to AuNPs only, scans 2 to 10 were at 2.5 min interval; dashed scan is after 50 min; (b)absorbance increase at 660 nm as a function of time for (◆) [Cys]=34 μM, [AcH]=5.5 mM; (●)[Cys]=34 μM, [AcH]=10 mM, see the spectra of (a), and (▼[Cys]=34 μM, [AcH]=5.5 mM, [Mn^{+2}]=0.12 mM; in all experiments the [AuNP]=0.85 nM.

The effect of Cys addition to stable Mn-AuNPs in aqueous acetic acid solutions is double. In one hand the replacement of citrate by Cys reduces the surface charge of gold nanoparticles. On the other hand, each adsorbed Cys molecule leaves the zwiterionic amino acid group facing outward from the nanoparticle surface, which can act as bridging linkers between one nanoparticle to another due to the strong electrostatic and/or H-bonding interactions. Both effects acting in the same direction strongly increase the self-assembly rate.

Attempts to disassemble the Cys-mediated aggregates by the addition of 12 μL of NaOH 1.0 M, final pH 8.2, did not show any appreciable effect. In fact, the rate for the reversal of the SPR band of homocysteine (similar to Cys) at pH 11.35, which is accompanied by a change in the color of the solution from bluish to red purplish, is very slow, nearly 9 days are required.[11]

Table 2. Experimental conditions and values of the first-order rate constants, k_o, k_1 and k_2, for surface plasmon resonance (SPR) band evolution of gold nanoparticles mediated by cysteine, captopril or S-nitrosocaptopril; ΔA refers to the net absorbance increase at the indicated wavelength for [AuNPs]=0.85 nM.

Cysteine (Cys)-mediated nanoparticles aggregation					
[Cys]/μM	[AcH]/mM	[Mn^{+2}]/mM	$k_o/10^{-3}s^{-1}$	---	$\Delta A_{(660\ nm)}$
14[a]	---	---	0.050	---	---
17	10	---	1.14	---	0.379
34	10	---	1.27	---	0.388
42.5	10	---	1.58	---	0.364
34	5.5	0.12	6.20	---	0.352
34	5.5	---	0.555	---	0.393
42.5	10	0.12	9.44	---	0.351
0.034	10	0.12	0.330	---	0.173
Captopril (cap)-mediated nanoparticles aggregation					
[cap]/mM			$k_1/10^{-3}s^{-1}$[b]	$k_2/10^{-3}s^{-1}$[b]	$\Delta A_{(610\ nm)}$
1.24	---	0.12	~0	0.35	0.439
1.13	10	0.12	~0	1.05	0.452
0.75	10	0.12	~0	0.78	0.427
0.75	10	…	1.18	0.28	0.434
0.38	10	0.12	1.76	0.21	0.398
0.75	5.5	---	1.6	0.17	0.453
0.75	5.5	0.12	3.25	0.73	0.456
S-Nitrosocaptopril (NOcap)-mediated nanoparticles aggregation					
[NOcap]/mM			$k_o/10^{-3}s^{-1}$	---	$\Delta A_{(610\ nm)}$
0.75	10	---	1.69	---	0.365
0.75	10	0.12	4.05	---	0.317
0.40	10	---	0.436	---	0.363
0.20	10	---	0.360	---	0.352
0.40	10[c]	---	0.495	---	0.720[c]
0.75	---	0.12	0.206	---	0.320

[a]Taken from ref. (12); [b]See Scheme 2 for their definition, the A-t data were fitted to $A=A_\infty+c_1\cdot exp(-k_1t)+c_2\cdot exp(-k_2t)$ with c_1 and c_2 being constants; [c]at [AuNPs]=1.7 nM.

3.Reversible assembly of gold nanoparticles mediated by captopril- and S-nitrosocaptopril.

The captopril molecule is a mercapto-proline derivative that contains the carboxylic group (pK_1=3.52) of the proline moiety and the thiol group (pK_2=10.00) of the propionyl residue. Thiols adsorb as their thiolate forms on gold surfaces.[27]

A recent study shows that the pK_a of sulfur-bound hydrogens of thiols on gold nanoparticles can be reduced by more than 10 pK_a units; in fact, the SERS spectra indicate that the sulfur-bound hydrogen is completely deprotonated even at very low pH.[28]

Aqueous solutions of citrate-capped gold nanoparticles 0.85 nM have a pH=6.20. At this pH, the carboxylic group of cap is ionized, whereas the thiol group is not. Under these conditions, addition of cap to aqueous solutions of gold nanoparticles does not show any change of the SPR band, at least in the time scale of these experiments. This fact does not mean cap molecules are not adsorbed on gold surface. Changes in the SPR band are observed

when the interaction between particles takes place, which is not possible between highly negative charged particles. Addition of 10 mM acetic acid induces cap-mediated assembly of AuNPs, and a new plasmon band centered at 620 nm develops.

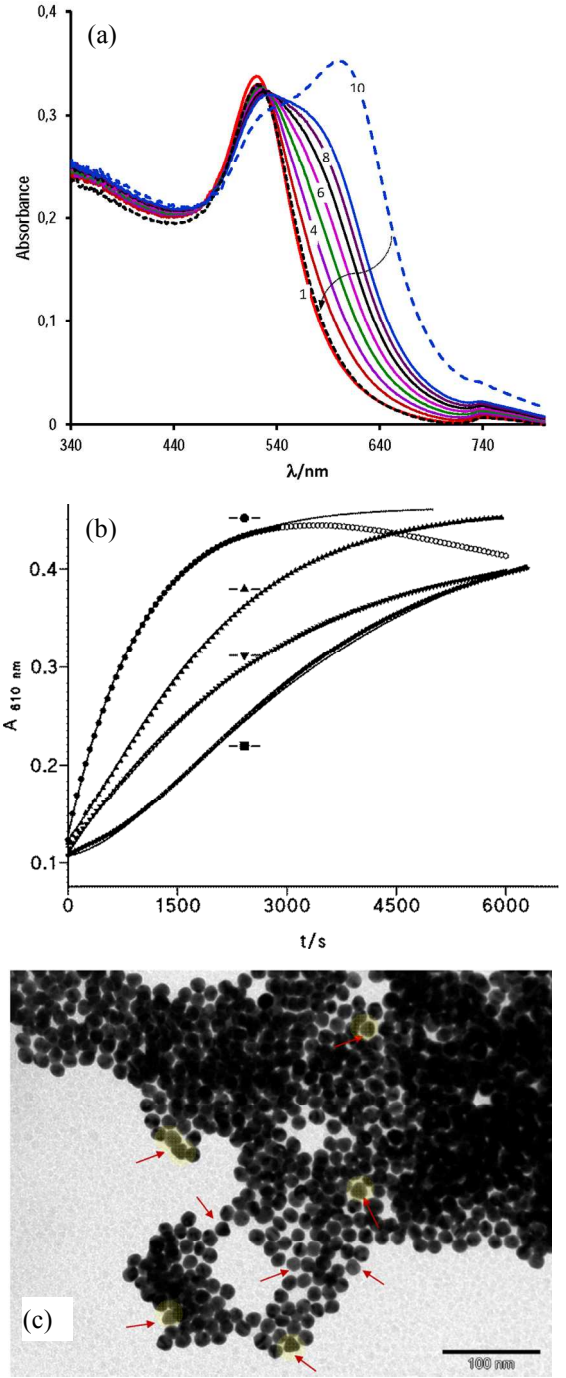

Figure 6. (a)Absorption spectrum of AuNPs in 10 mM AcH at [cap]=0.75 mM each 6 min; (- - -)after 120 min; (···)at the end of the reaction after adding 12μL NaOH 1 M; (b)increase absorbance as a function of time for [cap]=0.75 mM, [Mn^{+2}]=0.12 mM and [AcH] equal to (•)10 mM: the uppermost curve -fitted to first-order integrated rate equation, open circles not included- or to (▲)5.5mM -solid line fits double exponential-, and (▼)[cap]=1.24 mM; [Mn^{+2}]=0.12 mM; solid line fits first-order integrated rate equation; (■)cap]=0.75 mM; [AcH]=10 mM: the lowest curve, solid line fits double exponential; **(c)**TEM image for AuNPs in the presence of [cap]=1.1 mM and 10 mM acetic acid after 60 min.

Figure 6(a) shows the corresponding time evolution spectra, in which the dashed spectrum was taken after 2 h incubation; at this moment, the addition of 12 μL of NaOH 1 M (total vol. 1 mL, final pH 8.2) yields the dotted spectrum (follow the arrow) that matches spectrum 1 recorded in the absence of cap. This fact evidences the complete reversible of assembly cap-mediated process. The TEM image of this solution (after adding NaOH) resembles that shown in Fig. 1(c), i.e. no evidence of aggregation was observed; by contrast, the transmission electron microscopy image taken after 60 min incubation of AuNPs with cap in 5.5 mM acetic acid medium, indicates fully aggregation of both spherical and triangular gold nanoparticles, as it can be seen in Fig. 6(c).

The presence of small amount of Mn^{+2} ions, as low as 0.12 mM, facilitates the crosslinking process between gold nanoparticles, but the coexistence of both additives, i.e. Mn^{+2} ions in mild acid medium ([Mn^{+2}]=0.12 mM in 10 mM acetic acid) yields the most favorable conditions of visible interactions of cap-mediated gold nanoparticles assembly.

As for Cys, captopril molecules replace citrate from the gold surface due to the formation of strong covalent bonds S-Au. This fact disrupts the negatively charged citrate shell of AuNP and decreases the gold nanoparticle stability. The bulkier cap molecule than Cys makes the cap adsorption to gold surface much slower than with Cys, and high [cap] is required to observe interaction between AuNPs; in fact kinetic profiles of cap-mediated nanoparticle aggregation show induction period under some experimental conditions. On the other hand, the carboxyl group of adsorbed cap molecules remains exposed outward the NPs surface and favors nanoparticle interactions *via* hydrogen-bonding. By deprotonating these carboxyl groups, e.g. by adding NaOH, the H-bonds are broken as well and, consequently, the process is reverted.

The plot of the increase absorbance (A) with time (t) under different experimental conditions, showing the comparative effect of additives, is depicted in Fig. 6(b). We must indicate that the last additive to the sample was the Mn^{+2} ions and/or acetic acid; therefore, the possible binding of cap molecules to AuNPs-surface was allowed prior to the aggregation starts. High concentrations of either Mn^{+2} or acid results in A-t profiles that fit first-order integrated rate equation, whereas at low acid or in the absence of Mn^{+2} the kinetic profiles shows induction period.[29] These profiles can be interpreted as consecutive processes due to 1)binding of cap to gold nanoparticles with rate constant k_1 and 2)aggregation of nanoparticles due to hydrogen bonding interactions between the surface carboxyl groups of cap of adjacent nanoparticles of rate constant k_2, see Scheme 3. As H-bonding interactions are weaker than electrostatic interactions, the cap concentrations required to observed nanoparticles assembly are higher than cysteine concentration; in addition, the observed rate constant of the assembly process is higher in the case of Cys than the corresponding values of cap, compare k_o and k_2 in Table 2.

From the uppermost curve in Fig. 6(b), one can see that cap-capped gold nanoparticles are unstable (absorbance decreases at *ca* t>3000 s) and coalesce. The solution changes from blue to colorless and the aggregates stay at the bottom of the cuvette; but by adding NaOH to final pH 8.2 (12 μL NaOH 1 M) the

aggregates redisolve instantaneously and the solution becomes red, like well dispersed citrate-capped AuNPs.

Similar response to the addition of NaOH was observed in the disassembly of AuNPs aggregates mediated by glutathione; nevertheless, the degree of SPR band reversal is not completed. In a similar manner, addition of citrate to the GSH-AuNPs assembly after certain reaction time, the spectral evolution of SPR band can be prevented for further progression, frozen or slowly reverted depending on citrate concentration.[30] Kim *et al.* demonstrates that Pb^{+2} also mediated aggregation of gold nanoparticles capped with 11-mercaptoundecanoic acid, and addition of EDTA partially reverses the response due to Pb^{+2} chelation.[31] In the same sense, the SPR band of AuNPs aggregation mediated by PEN or NAP is pH dependent and the assembly-disassembly process demonstrates to be fully reversible when the pH was cycled between 7 and 3.[16]

Finally, we analyze the interaction of S-nitrosocaptopril, NOcap, with colloidal gold solutions. The only structural difference between cap and NOcap is the replacement of –SH in cap by –SNO in NOcap, which allow us information of sulfur-gold interaction.

In aqueous acid medium of sodium nitrite, captopril is readily converted to S-nitrosocaptopril. The UV-vis spectrum of NOcap aqueous solutions shows the characteristic band at 332 nm (ε=1020 $M^{-1}cm^{-1}$) and a much less intense absorption band centered at 547 nm (ε=20 $M^{-1}cm^{-1}$).[21]

S-Nitrosothiols (RSNOs) release NO in the presence of AuNPs because of the affinity between gold and thiols, which catalysed and tuned the NO deliver process because of the affinity between gold and thiols, as shows an interesting study by Hervés *et al.*[32] The available Au-surface determines the released amount of NO. By employing a sensitive NO electrode, the stoichiometry of the reaction was estimated and the results indicate that the amount of NO released is not quantitative at low concentration of AuNPs. The rate equation is zero-order with respect to [RSNO] and first-order on [AuNPs], and the reactivities of the different RSNO analysed, which include the nitrosothiols of PA, N-acetylpenicillamine, and GSH, towards the Au-surface are quite similar with rate constants of the order of ~5×10^{-2} s^{-1}.

Figure 7(a) shows the reaction spectra of nanoparticle assembly mediated by S-nitrosocaptopril. The band centered at 332 nm is due to NOcap, characteristic of RSNOs. The SPR band of aqueous citrate-capped gold nanoparticles centered at 520 nm shifts to 620 nm in the presence of NOcap, i. e., the reaction spectra within 440-800 nm interval of NOcap-mediated assembly is not different from that of AuNPs aggregation by cap, as expected, due to cap molecules are immobilized on the gold surface by strong S-Au bonds. The green dashed spectrum, which matches that at zero time, was recorded once the reaction was completed (after ~60 min) and just after adding 12 µL of NaOH 1 M to the reaction sample. The result evidences the reverse of the gold nanoparticles aggregation process.

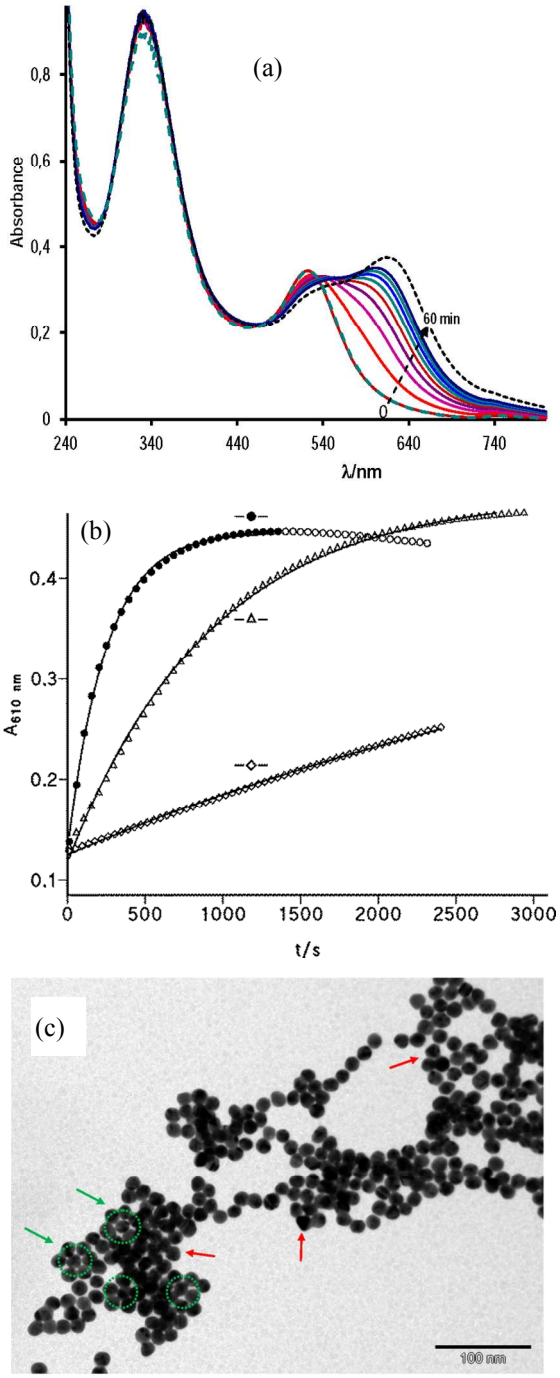

Figure 7.(a)UV-vis Absorption spectra of AuNPs 0.85 nM in 10 mM acetic acid and [NOcap]=0.75 mM recorded at 6 min interval; (- - -)after 120 min; (⋯)at the end of the reaction after adding 12µL NaOH 1 M (b)Increase absorbance with time of AuNPs in the presence of [NOcap]=0.755 mM at (•)[AcH]=10 mM, and [Mn^{+2}]=0.12 mM, open circles not included in the fitting process; (△)[AcH]=10 mM, and (◇)[Mn^{+2}]= 0.12 mM; **(c)**TEM image of AuNPs incubated during 40 min with 0.75 mM NOcap at 10 mM acetic acid and 0.12 mM Mn^{+2}.

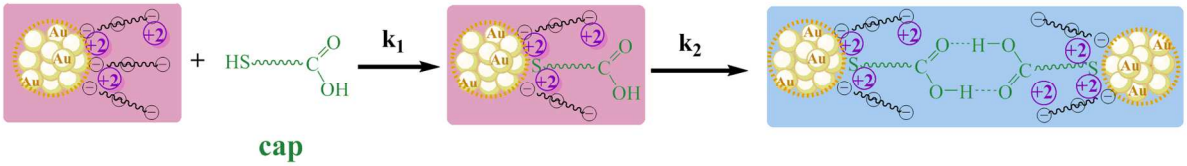

Scheme 3. Schematic representation of cap adsorption on Mn-AuNPs, color change after aggregation, and H-bonding between adjacent nanoparticles

Figure 7(b) shows the effect of acetic acid and Mn^{+2} ions concentration on the rate of AuNPs assembly mediated by NOcap. The presence of 0.12 mM of Mn^{+2} accelerates the reaction; the catalytic effect is much more marked in 10 mM acetic acid, but the coexistence of both additives makes the reaction goes to the end in a few minutes. In every case the absorbance-time profiles fit the first-order integrated rate equation. Values of the observed rate constant, k_o, are listed in Table 2 along with the corresponding experimental conditions. The comparison of k_o with the equivalent rate constant, k_2, for cap-mediated aggregation evidences the accelerating effect of NOcap.

The NOcap-mediated assembly of AuNPs shows good first-order kinetics under all the experimental conditions studied, in other words, the binding of NOcap molecules to gold NPs is much faster than the nanoparticles aggregation, contrarily to that observed with cap, that is, gold nanoparticles stabilized by NOcap seem to reach equilibrium faster (step 1 in Scheme 3) than those stabilized with cap. The only difference between cap and NOcap is the –S-H bond in cap against –S-NO in NOcap. Literature results show that S-nitrosothiols decomposition occurs through thermal homolysis of the RS-NO bond.[33] The RS-NO homolytic dissociation energies (around 20-30 kcal/mol) are remarkably lower than heterolysis cleveage by an average of 29 kcal.[34] The gold thiolate (S-Au) bond energy is about 40 kcal/mol,[35] i.e. greater than that of RS-NO bond. Hence, the RS-NO bond can be easily cleaved in the presence of AuNPs that favors S-Au bond formation. Therefore, citrate capped gold nanoparticles enhance the NO release rate from S-nitrosothiol based systems, being modulated by affecting the size and concentration of gold nanoparticles.[33, 36]

On the other hand, RS-H bond energy is about 87 kcal/mol,[35] i. e. much greater than that of RS-Au bond. Consequently, the thiol must adsorb on gold surface in the thiolate form,[27] whose concentration at acidic pH is quite small, a fact that explain the slow reaction rate of cap adsorption against NOcap.

The TEM analysis of the samples confirmed that at neutral and basic pH the particles are well-dispersed and randomly distributed on the TEM grid, while in 10 mM acetic acid or in the presence of a small amount of manganese ions the particles tend to coalesce as it is shown in Fig. 7(c) for NOcap-mediated assembly. Notice the abundance of symmetrical arrangements of spherical and triangular gold nanoparticles.

In summary, aqueous solutions of 0.85 nM AuNPs and 10 mM acetic acid have a pH around 4.40; but, as the thiol group of Cys or cap binds to gold surface, the releasing protons fall the pH to around 3.5. At this pH, the amine group of Cys is protonated and the carboxyl group is ionized, while the carboxyl groups of either cap or NOcap are partially protonated. This important fact evidences the existence of electrostatic interactions in Cys-modified gold nanoparticles, and H-bonding interations in cap (or NOcap) mediated gold nanoparticles aggregation. Therefore, as NOcap –or cysteine or captopril– is going to exchange by citrate-capped gold NPs, the pH of the solution decreases and the particles tend to aggregate, leading to plasmon coupling, which results in broadening and red-shift of the maximum absorption, being the maximum observed wavelength around 672 nm in the Mn^{+2}-mediated aggregation; 660 nm with Cys, and 620 nm with cap or NOcap, as average values because the many factors that condition λ_{max} make precise shape of the new bands may vary even from sample to sample. Actually it is well established that the origin of manoparticle aggregation in these systems is the strong interaction gold-sulfur or due to a strong reduction in zeta potential at high concentration of manganese ions. Consequently, we assume that Cys, cap or NOcap are immobilized on the gold surface via the thiolate group. Therefore, the stability of Cys –or cap or NOcap– modified AuNPs will be determined by the interactions of amine and/or carboxylic groups exposed to the exterior surface of NPs.

Conclusions

The presence of small amounts of Mn^{+2} ions in mild acid medium has proven to dramatic accelerate the assembly of thiol-capped gold nanoparticles obtained through ligand exchange is aqueous solution. The two mechanisms proposed to explain nanoparticle assembly have been observed in this study. The assembly via electrostatic interactions between zwitterionic amino acids is operative when using cysteine as the ligand; the process results irreversible on increasing pH to the basic region, and the kinetics show first-order behaviour with rate constants strongly dependent on the concentration of both the acid and the manganese ions. The assembly via hydrogen bonding is proposed when the ligand is captopril or S-nitrosocaptopril. In contrast to that observed with Cys, the process is fully reversibly when the pH is increased to basic levels, a fact that proves the stronger electrostatic interactions than H-bonding. The aggregation rate was found to be significantly higher for NOcap than for cap, showing the important role that plays the specific nature of the ligand molecule, which, in the present case, can be explained taking into account the bond energies of both the broken and formed bonds. Kinetics of the assembly process show first-order behaviour with NOcap under all tested conditions, while with cap consecutive reactions appear to occur at low concentration or either acid or cap.

Acknowledgements

We are indebted to Dr. Sarah Fiol and Dr. Juan Antelo, of the University of Santiago de Compostela (Instituto de Investigaciones Tecnológicas) for their assistance in the measurement of ζ-potentials.

Notes and references

[a] *Departamento de Química Física e E. Q. I. Facultade de Ciencias. Universidad de La Coruña. 15071-A Coruña (SPAIN).*
emilia.iglesias@udc.es
[b] *Departamento de Química Física. Facultad de Química. Universidad de Sevilla. 41012–Sevilla (SPAIN)*

1. M- E. Stewart, C. R. Anderton, L. B. Thompson, J. Maria, S. K.Gray, J. A. Rogers, R. G. Nuzzo,. *Chem. Rev.* 2008**, 108,** 494-521.
2. C. M. Cobley, J. Chen, E. C. Cho, L. V. Wang, Y. Xia, *Chem. Soc. Rev.*, 2011, **40**, 44–56
3. K. Saha, S. S. Agasti, C. Kim, X. Li, V. M. Rotello, *Chem. Rev.* 2012**, 112**, 2739−2779.
4. H. Jans, Q. Huo, C*hem. Soc. Rev.,* 2012, **41,** 2849-2866.

5. S. Zeng, D. Baillargeat, H.-P. Ho, K.-T. Yong, *Chem. Soc. Rev.,* 2014, **43**, 3426-3452
6. V. Myroshnychenko, J. Rodríguez-Fernández, I. Pastoriza-Santos, M. A. Funston, C. Novo, P. Mulvaney, L. M. Liz-Marzán, F. J. García de Abajo. *Chem. Soc. Rev*., 2008, **37***,* 1792–1805
7. J. Turkevich, P. C. Stevenson, J. A. Hillier, *Discuss. Faraday Soc.*, 1951, **11,** 55-75.
8. J. Kimling, M. Maier, B. Okenve, V. Kotaidis, H. Ballot, A. Plench, *J. Phys. Chem. B*, 2006, **110**, 15700-15707.
9. D. C. Hone, A. H. Haines, D. A. Russell, *Langmuir*, **2003**, *19*, 7141-7144.
10. K. J. Fahnestock, M. Manesse, H. A. McIlwee, C. I. Schauer, R. Boukherroub, S. Szunerits, *Analyst,* 2009, **134,** 881-886.
11. I.-I. S. Lim, W. Ip, E. Crew, P. M. Njoki, D. Mott, C.-J. Zhong, Y. Pan, Z. Zhou, *Langmuir*, 2007, **23**, 826-833
12. F. X. Zhang, I. Han, I. B. Israel, J. G. Daras, M. M. Maye, N. K. Ly, C.-J. Zhong, *Analyst*, 2002, **127**, 462-465.
13. L. Li, B. Li, *Analyst*, 2009, **134**, 1361-1365
14. B. Hu, X. Cao, P. Zhang, *New J. Chem.* 2013, **37**, 3853-3856.
15. S. Basu, S. Panigrahi, S. Praharaj, S. K. Ghosh, S. Pande, S. Jana, T. Pal, *New J. Chem.* 2006, **30**, 1333-1339.
16. P. Taladriz-Blanco, N. J. Buurma, L. Rodríguez-Lorenzo, J. Pérez-Juste, L. M. Liz-Marzán, P. Hervés, *J. Mater. Chem.*, 2011, **21**, 16880-16887.
17. H. M. Zakaria, A. Shah, M. Konieczny, J. A. Hoffmann, A. J. Nijdam, M. E. Reeves, *Langmuir*, 2013, **29**, 7661−7673.
18. Z. Zhong, S. Patskovskyy, P. Bouvrette, J. Luong, A. Gedanken, *J. Phys. Chem. B* 2004, **108**, 4046−4052.
19. R. Stewart, The proton applications to organic chemistry. Academic Press: London. 1985.
20. S. G. Tajc, B. S. Tolbert, R. Basavappa, B. L. Miller, *J. Am. Chem. Soc.*, 2004, **126,** 10508-10509.
21. A. Sexto, E. Iglesias, *Org. Biomol. Chem.*, 2011, **9**, 7207-7216
22. J. Loscalzo, D. Smick, N. Andon, J. S. Cooke, *J. Pharmacol. Exp. Ther.*, 1989, **249**, 726-729.
23. Addition of 0.074 mM of acetic acid to a colloidal gold solution 18.7 nm at pH 3 (adjusted by dropwise addition of HCl) does not cause the aggregation of gold after as long as 1000 min incubation, according to the data of ref. 17.
24. K. J. Laidler, *Chemical Kinetics*. 3rd Edition. Harper Collins Publishers. 1987. Ch. 6.
25. E. H. Murph, S. Jacobs, J. Liu, T. C. C. Hu, M. Siegfired, S. M. Serkiz, J. Hudson, *J. Nanopart Res*. 2012**, 14**. 658-669.
26. P. K. Sudeep, S. T. S. Joseph, K. G. Thomas, *J. Am. Chem. Soc.*, 2005, **127**, 6516-6517.
27. J. E. Mattiesen, D. Jose, C. M. Sorensen, K. I. Klabunde, *J. Am. Chem. Soc.*, 2012, **134,** 9376-9379, and references therein.
28. S. M. Ansar, G. S. Perera, D. Jiang, R. A. Holler, D. Zhang, *J. Phys. Chem. C*, 2013, **117**, 8793-8798.
29. Espenson. J. H. Chemical Kinetics and Reaction Mechanisms, 2nd ed., 1995, McGraw-Hill, ch. 4.
30. I.-I. S. Lim, D. Mott, W. Ip, P. M. Njoki, Y. Pan, S. Zhou, C.-J. Zhong, *Langmuir*, 2008, **24,** 8857-8863.
31. Y. Kim, R. C. Johnson, J. T. Hupp, *Nano Letters,* 2001, **1**, 165-167.
32. P. Taladriz-Blanco, V. Pastoriza-Santos, J. Pérez-Juste, P. Hervés, *Langmuir*, 2013, **29**, 8061-8069.
33. M. D. Bartberger, J. M. Mannion, S. C. Powel, J. S. Stamler, K. N. Houk, E. J. Toone, *J. Am. Chem. Soc.*, 2001, **123***,* 8868-8869.
34. J.-M. Lu, J.M. Wittbrodt, K. Wang, Z. Wen, H.B. Schlegel, P. G. Wang, J.-P. Cheng, *J. Am. Chem. Soc.*, 2001, **123***,* 2903-2904
35. A. Ulman, *Chem. Rev.*, 1996, **96**, 1533-1554.
36. S. Priya, T. Kaviyarasan, S. Berchmans, *Analyst*, 2012, **137**, 1541-1543.